On a Vehicular Suspension for a Non-ideal and Nonlinear Orchard Tower Sprayer Through an Inverted Pendulum Using Reologic Magneto (MR)

R. N. Silva, J. L. P. Felix, Jose Manoel Balthazar, A. M. Tusset, M. A. Ribeiro, W. B. Lenz, and A. Cunha

Abstract In this paper, analysis of the nonlinear dynamics responses of a structure equipped with a vehicle suspension that uses a fluid with magneto rheological characteristics to control the possible instability and chaotic motion. It is a spray orchards of tower type, with an unbalanced electric motor (Non-ideal) located at the top of the tower representing the concentrated mass of their fans, which represents the real system the best way possible. The simulations show that the MR suspension reduce the amplitude of oscillations of all the masses of the system, being the most important the mass of the cart and fans. The influence of the non- ideal motor is important to check the influence of a possible imbalance of fans.

Keywords Spray orchards type tower · Nonlinear dynamics · Non-ideal system · Vehicle suspension · Magneto- Rheological fluid damper

1 Theoretical Mathematical Model of the Tower-Type Orchard Sprayer

The study of the [6, 8] nonlinear dynamics of an agricultural tower pulverizer, coupled with a vehicle suspension, that is subject to random excitations due to soil irregularities, modeled as an inverted double pendulum over a moving suspension, with three degrees of freedom (one translation and two rotations). To take into account the random loadings, a parametric probabilistic approach was employed, where the external force was assumed to be a harmonic random process with random amplitude and frequency. The probability distribution of these random [8] parameters was

R. N. Silva (✉) · J. M. Balthazar · A. M. Tusset · M. A. Ribeiro · W. B. Lenz
Federal Technological University of Paraná, Campus Ponta Grossa, PR, Brazil

J. M. Balthazar
Faculty of Mechanical Engineering of Bauru, São Paulo State University, Bauru, SP, Brazil

A. Cunha
Institute of Mathematics and Statistics, Rio de Janeiro State University, Rio de Janeiro, RJ, Brazil

J. L. P. Felix
Federal University of Southern Frontier -UFFS, Cerro Largo, RS, Brazil

J. M. Balthazar (ed.), *Nonlinear Vibrations Excited by Limited Power Sources*,
Mechanisms and Machine Science 116, https://doi.org/10.1007/978-3-030-96603-4_10

constructed based on the known information through the maximum entropy principle. The results of numerical simulation show that large discrepancies in the system response can be seen when one compares the mean of the stochastic model with the nominal (deterministic) model. It is also noted that these responses are subject to a high level of uncertainty. Furthermore, an analysis of the system response probability distributions [6, 8] shows that they present asymmetries with respect to mean and unimodal behavior.

Some considerations were taken to arrive at the theoretical model. Initially, the simplifications [14, 15] will be considered. Where, initially, all the masses (truck, axle, wheel and tower with its eight fans) are concentrated in their centers of gravity. One of the main simplifications to be considered is that the operation of the sprayer will take place in short periods of time, because if long periods are taken the mass of the reservoir tank will have its center of gravity shifted, due to the fact that the sprayer starts the work with the reservoir full of defensive liquid and it is discharging during the spraying operation, until it finishes empty. Therefore, the mass of the reservoir tank is considered constant.

Once this is done, the reservoir mass and the chassis mass are grouped into a single invariant center of gravity m_2. All the concentrated masses of the eight fans are replaced by a single mass which, added to the motor mass, results in m_3, and the unbalanced mass of the direct current electric motor is m_0, located at the top of the tower. The tower, in turn, is represented by a negligible mass element of length L_2. The pivot point of the tower is represented by a point P, located at a distance L_1 above the trailer's center of gravity. This same junction P is represented by an elastic element k_t and damping c_t torsional and linear.

Starting from the premise that, when the system rotates around the point of concentrated mass m_2, the left and right tires have the same displacement, in opposite directions; thus, it is considered that the system only presents a translational movement in the vertical direction. Therefore, the theoretical system can be considered as being of ¼ of a vehicle or quarter-car, taking into account the displacement of only one of the wheels. This wheel is then represented by an element of mass *m1* with linear stiffness k_1. And a vehicle-type MR damper, represented by F, is coupled to the system, in parallel to the viscous spring-damper suspension k_2 and c, respectively, according to the Bounc-Wen model.

An X–Y coordinate system is adopted, with X at ground level and Y passing through the center of mass of truck m_2. The tower will then have an angular offset ϕ_1. It is the angular displacement of the unbalanced mass is ϕ_2. Excitements resulting from irregularities presented by the soil of the orchards cause displacements in the tires represented by ye_1; mathematically ye_1 represents an excitation source that can be of the harmonic, transient, etc. type.

However, it is observed that in the simplification presented the model presented has four degrees of freedom, with only the mass of the fans concentrated at the top of the tower, called m_2 in the figure, and without taking in considering the mass of the wheels. Finally, the next simplification will be to add the unbalanced mass engine at the top of the tower and also the mass of a wheel, thus transforming the model

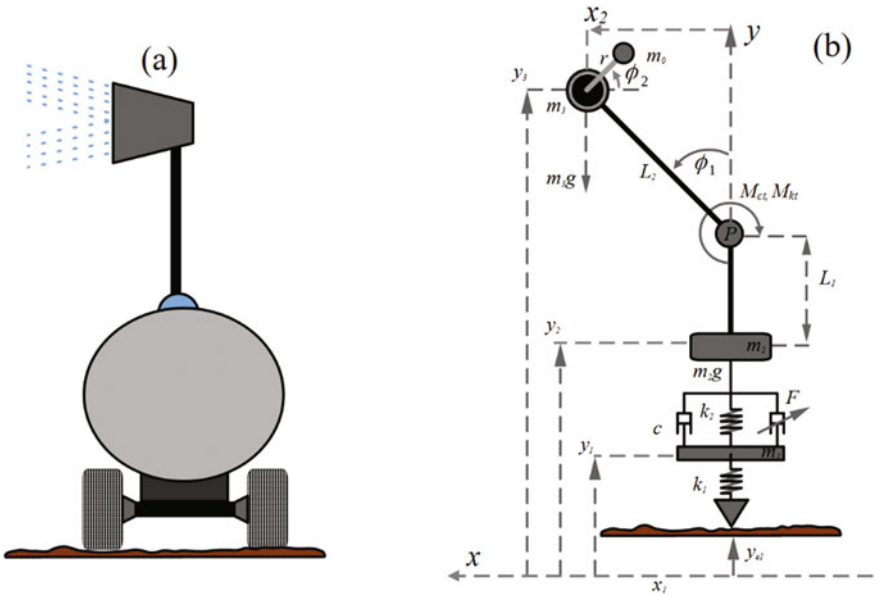

Fig. 1 Theoretical mathematical model of the turret sprayer. **a** trailer and tower coupled and **b** scheme of forces applied

into a ¼ vehicle (Quarter-car). Finally, all the simplifications mentioned above are represented in a theoretical scheme presented in the following figure, Fig. 1.

The differential equations of motion are obtained from the Method of Energies and Conservative Forces, which is employed using the so-called Euler–Lagrange Equations.

2 Euler–Lagrange Energy Method

Euler–Lagrange equation is defined as:

$$\frac{d}{dt}\left(\frac{\partial L}{\partial \dot{q}_j}\right) - \frac{\partial L}{\partial q_j} = Q_j \tag{1}$$

with j = 1,2,3…. Where $L = T_T - V_T$, called Lagrangian where T_T represents the total kinetic energy of the system, V_T is the work of conservative forces (potential energy of the chassis, tower and unbalanced motor masses, and the potential energy of the elastic elements). And Q is the work of all non-conservative forces (such as the energy dissipated by the damping elements).

2.1 Total Kinetic Energy of the System

The total kinetic energy of the T_T system is the sum of the kinetic energy portions of the trailer, the tower, the unbalanced mass of the engine, and the tire, which are represented by $T_c,\ T_t,\ T_o\ and\ T_p$ respectively. T_T is then defined as:

$$T_T = T_p + T_c + T_t + T_0 \tag{2}$$

Where:

$$T_p = \frac{1}{2}m_1 V_1^2 = \frac{1}{2}m_1\left(\dot{x}_1^2 + \dot{y}_1^2\right) \tag{3}$$

$$T_c = \frac{1}{2}m_2 V_2^2 = \frac{1}{2}m_2(\dot{x}_1^2 + \dot{y}_2^2) \tag{4}$$

$$T_t = \frac{1}{2}(m_3)V_3^2 = \frac{1}{2}(m_3)\left(\dot{x}_2^2 + \dot{y}_3^2\right) + \frac{1}{2}m_3 L_2^2\dot{\phi}_1^2 \tag{5}$$

With $m_3 = M + m$, where M represents the concentrated mass of the fans and m the mass of the motor. The term $m_3 L_2^2$ in Eq. 5 represents the moment of inertia of the tower.

$$T_o = \frac{1}{2}m_0\left(\dot{x}_0^2 + \dot{y}_0^2\right) + \frac{1}{2}m_0 r^2\dot{\phi}_2^2 \tag{6}$$

The horizontal and vertical positions of the m_3 tower mass are given as follows, respectively: The horizontal position is:

$$\begin{aligned} x_2 &= L_2 sin\phi_1 - x_1 \\ x_2 &= L_2 sin\phi_1 - x_1 \end{aligned} \tag{7}$$

and its first and second derivatives, respectively in time:

$$\begin{aligned} \dot{x}_2 &= L_2\dot{\phi}_1 cos\phi_1 - \dot{x}_1 \\ \ddot{x}_2 &= \ddot{x}_1 L_2\ddot{\phi}_1 cos\phi_1 - L_2\phi_1^2 sin\phi_1 \end{aligned}$$

The vertical position is:

$$y_3 = y_2 + L_1 + L_2 cos\phi_1 \tag{8}$$

and its first and second derivatives, respectively in time:

$$\dot{y}_3 = \dot{y}_2 + L_1 + L_2\dot{\phi}_1 sin\phi_1$$

$$\ddot{y}_3 = \ddot{y}_2 - L_2\ddot{\phi}_1 sin\phi_1 - L_2\dot{\phi}_1^2 cos\phi_1$$

The horizontal and vertical positions of the unbalanced mass m_0 can be described as follows:

$$x_0 = L_2 sin\phi_1 - rcos\phi_2 \tag{9}$$

$$y_0 = L_2 cos\phi_1 - rsin\phi_2 + L_1 + y_2 \tag{10}$$

With its derivatives $\dot{x}_0$ and $\dot{y}_0$ in time given by:

$$\dot{x}_0 = \dot{\phi}_1 L_2 cos + \dot{\phi}_2 rsin\phi_2$$
$$\dot{y}_0 = -\dot{\phi}_1 L_2 sin\phi_1 + \dot{\phi}_2 rcos\phi_2 + \dot{y}_2$$

representing the coordinates of the angular velocity of the unbalanced mass m0.

In this way, substituting Eqs. 3–6 in Eq. 2, we obtain:

$$\begin{aligned} T_t = {} & \tfrac{1}{2}m_1\left(\dot{x}_1^2 + \dot{y}_1^2\right) + \tfrac{1}{2}m_2\left(\dot{x}_1^2 + \dot{y}_2^2\right) + \tfrac{1}{2}m_3\left(\dot{x}_2^2 + \dot{y}_3^2\right) \\ & + \tfrac{1}{2}m_3 L_2^2\dot{\phi}_1^2 + \tfrac{1}{2}m_0\left(\dot{x}_0^2 + \dot{y}_0^2\right) + \tfrac{1}{2}m_0 r^2\dot{\phi}_2^2 \end{aligned} \tag{11}$$

with respect to time of Eqs. 7 and 8 in the previous Eq. 11, we have:

$$\begin{aligned} T_t = {} & \frac{1}{2}m_1\dot{x}_1^2 + \frac{1}{2}m_1\dot{y}_1^2 + \frac{1}{2}m_2\dot{x}_1^2 + \frac{1}{2}m_2\dot{y}_2^2 + \\ & \frac{1}{2}m_0\left(\dot{x}_0^2 + \dot{y}_0^2\right) + \frac{1}{2}m_3 L_2^2\dot{\phi}_1^2 + \frac{1}{2}m_0 r^2\dot{\phi}_2^2 \\ & \frac{1}{2}m_3\left(\dot{x}_1 + L_2\dot{\phi}_1 cos\phi_1\right)^2 + \frac{1}{2}m_3\left(\dot{y}_2 - L_2\dot{\phi}_1 sin\phi_1\right)^2 + \end{aligned} \tag{12}$$

And now the first time derivatives of Eqs. 9 and 10 in Eq. 12, you get:

$$\begin{aligned} T_T = {} & \frac{1}{2}m_1\dot{x}_1^2 + \frac{1}{2}m_1\dot{y}_1^2 + \frac{1}{2}m_2\dot{x}_1^2 + \frac{1}{2}m_2\dot{y}_2^2 \\ & + \frac{1}{2}m_3\left(\dot{x}_1 + L_2\dot{\phi}_1 cos\phi_1\right)^2 + \frac{1}{2}m_3\left(\dot{y}_2 - L_2\dot{\phi}_1 sin\phi_1\right)^2 + \\ & \frac{1}{2}m_0\left(\dot{\phi}_1 L_2 cos\phi_1 + \dot{\phi}_2 rsin\phi_2\right)^2 + \frac{1}{2}m_3 L_2^2\dot{\phi}_1^2 + \frac{1}{2}m_0 r^2\dot{\phi}_2^2 \\ & \frac{1}{2}m_0\left(-\dot{\phi}_1 L_2 sin\phi_1 + \dot{\phi}_2 rcos\phi_2 + \dot{y}_2\right)^2 \end{aligned} \tag{13}$$

$$T_T = \frac{1}{2}m_3\dot{x}_1^2 + \frac{1}{2}m_3\dot{y}_2^2 - m_3\dot{x}_1 L_2\dot{\phi}_1 cos\phi_1 - m_3\dot{y}_2 L_2\dot{\phi}_1 sin\phi_1 +$$

$$\frac{1}{2}m_3L_2^2\dot{\phi}_1^2\left(cos^2\phi_1+sin^2\phi_1\right)+\frac{1}{2}m_0\dot{\phi}_1^2L_2^2\left(cos^2\phi_1+sin^2\phi_1\right)+$$
$$\frac{1}{2}m_0\dot{\phi}_2^2r^2\left(cos^2\phi_2+sin^2\phi_2\right)-$$
$$m_0\dot{\phi}_1\dot{\phi}_2L_2r(cos\phi_2sin\phi_1-cos\phi_1sin\phi_2)+$$
$$\frac{1}{2}m_0\dot{y}_2^2-m_0\dot{y}_2\dot{\phi}_1L_2sin\phi_1+m_0\dot{y}_2\dot{\phi}_2rcos\phi_2+$$
$$\frac{1}{2}m_1\dot{x}_1^2+\frac{1}{2}m_1\dot{y}_1^2+\frac{1}{2}m_2\dot{x}_1^2+\frac{1}{2}m_2\dot{y}_2^2+\frac{1}{2}m_3L_2^2\dot{\phi}_1^2+\frac{1}{2}m_0r^2\dot{\phi}_2^2 \tag{13b}$$

The lateral displacement of the trailer's center of gravity, x_1, limited by the tires, is very small compared to the magnitudes of the other displacements. Thus, it will be assumed that x_1 is constant [13]. So: if constant, then: if $x_1 \cong$ constant, then: $\dot{x}_1 \cong \ddot{x}_1 \cong 0$.

In this way, making use of the trigonometric identities below:

$$sin^2\phi_2+cos^2\phi_2=1$$

$$cos\phi_2cos\phi_1+sin\phi_1sin\phi_2=\cos(\phi_2-\phi_1)$$

we have the following equation for the total kinetic energy of the system:

$$T_T=\frac{1}{2}m_3\dot{y}_2^2-m_3\dot{y}_1L_2\dot{\phi}_1sin\phi_1+\frac{1}{2}m_3L_2^2\dot{\phi}_1^2+\frac{1}{2}m_0\dot{\phi}_1^2L_2^2$$
$$+\frac{1}{2}m_0r^2\dot{\phi}_2^2-m_0\dot{\phi}_1\dot{\phi}_2L_2r\cos(\phi_2-\phi_1)+\frac{1}{2}m_0\dot{y}_2^2-$$
$$m_0\dot{y}_2\dot{\phi}_1L_2sin\phi_1+m_0\dot{y}_2\dot{\phi}_2rcos\phi_2+\frac{1}{2}m_1\dot{y}_1^2+\frac{1}{2}m_2\dot{y}_2^2+$$
$$\frac{1}{2}m_3L_2^2\dot{\phi}_1^2+\frac{1}{2}m_0r^2\dot{\phi}_2^2 \tag{14}$$

$$T_T=\frac{1}{2}(m_2+m_3+m_0)\dot{y}_2^2-(m_3+m_0)L_2\dot{y}_2\dot{\phi}_1sin\phi_1+$$
$$m_3L_2^2\dot{\phi}_1^2+m_0r^2\dot{\phi}_2^2+m_0\dot{y}_2\dot{\phi}_2rcos\phi_2-$$
$$m_0r\dot{\phi}_1\dot{\phi}_2L_2\cos(\phi_2-\phi_1)+\frac{1}{2}m_1\dot{y}_1^2+\frac{1}{2}m_0L_2^2\dot{\phi}_1^2 \tag{14a}$$

2.2 Total Potential Energy of the System

The total potential energy of the system or the work of the conservative forces of the V_T system is given by the sum of the potential energy portions of the elastic elements of the K_1, K_2 and K_T system, as follows:

$$V_T = E_{Pk1} + E_{Pk2} + E_{PkT} \tag{15}$$

The previous potential energy equation can then be rewritten as follows:

$$V_T = \frac{1}{2}K_1\left(\Delta y_{K_1}\right)^2 + \frac{1}{2}K_2\left(\Delta y_{K_2}\right)^2 + \frac{1}{2}K_T\left(\Delta y_{K_T}\right)^2 \tag{16}$$

Replacing the appropriate displacements, Eqs. 8 and 10, we obtain the following equation:

$$V_T = \frac{1}{2}K_1(y_1 - y_{e1})^2 + \frac{1}{2}K_2(y_2 - y_1)^2 + \frac{1}{2}K_T\phi_1^2 \tag{17}$$

$$V_T = \frac{1}{2}K_1\left(y_1^2 - 2y_1y_{e1} + y_{e1}^2\right)^2 + \frac{1}{2}K_2\left(y_1^2 - 2y_1y_2 + y_1^2\right)^2 + \frac{1}{2}K_T\phi_1^2 \tag{17a}$$

From the previous equation (Eq. 17a), the effect of gravity as a conservative force was disregarded, due to its little influence on the response of the system.

2.3 Work of Non-Conserved Forces

The work of the non-conserved forces or total damping of the Q system represents the total energy dissipated by the damping elements, and is given by the sum of the energy dissipated by the suspension damper (F_c) and by the junction damper torsional (F_{c_T}), in addition to the energy dissipated by the damper with MR (F), as follows:

$$Q = F_c + F_{c_T} + F \tag{18}$$

So the previous equation is rewritten as follows:

$$Q = C(\Delta\dot{y}_C) + C_T(\Delta\dot{y}_{C_T}) + F \tag{19}$$

where the terms $\Delta\dot{y}_C$ and $\Delta\dot{y}_{C_T}$ represent the deformation velocities of the damping elements, respectively. And they are given as follows:

$$\Delta\dot{y}_C = \dot{y}_2 - \dot{y}_1 \tag{20}$$

$$\Delta\dot{y}_{C_T} = \dot{\phi}_1 \tag{21}$$

The strength of the MR damper is mathematically represented by the Bounce-Wen model. And then, replacing Eqs. 20 and 21 in 19, you can rewrite the expression for Q as follows:

$$Q = C(\dot{y}_2 - \dot{y}_1) + C_T\left(\dot{\phi}_1\right) + \alpha z \tag{22}$$

where *Va* is the supply voltage, i_a is the supply current, Φ is the magnetic flux and φ is the angular position of the motor [12].

$$L_a \frac{di_a}{dt} + R_a i_a + E_b = V_a \tag{23}$$

where *Eb* is the counter-electromotive force between the motor armature terminals given by:

$E_b = k_E \frac{d\phi_2}{dt}$ where k_E is the motor voltage constant and ϕ_2 the motor angular position. Also according to [12], to study the interaction between the tower and the motor, the direct current motor is considered in a simplified way, and therefore the torque generated by the motor can be expressed as follows:

$$M_m = \hat{a} - \hat{b}\dot{\phi}_2 \tag{24}$$

where parameter $\hat{a}$ is related to the electrical voltage applied to the direct current motor and $\hat{b}$ related to the type of motor used, both defined as follows, respectively:

$$\hat{a} = \frac{k_m V_a}{R_a} \tag{25}$$

$$\hat{b} = \frac{k_m k_b}{R_a} \tag{26}$$

where R_a is the motor electrical resistance, k_b the motor voltage constant, V_a the input voltage applied to the motor armature, k_m is the motor torque constant.

Then, replacing Eq. 24, rewrite Eq. 22 as follows:

$$Q = C(\dot{y}_2 - \dot{y}_1) + C_T\left(\dot{\phi}_1\right) + \alpha z + \hat{a} - \hat{b}\dot{\phi}_2 \tag{27}$$

2.4 Application of the Euler–Lagrange Equation

The Lagrangian of the system under study is calculated by the difference between the total kinetic energy, the total potential energy and the dissipation energy of the system, is $L = T_T - V_T$. The Lagrangian is then obtained through the difference between Eqs. 7, 10 which results in [5]

$$L = \frac{1}{2}(m_2 + m_3 + m_0)\dot{y}_2^2 - (m_3 + m_0)L_2\dot{y}_2\dot{\phi}_1 sin\phi_1 + m_3 L_2^2\dot{\phi}_1^2 + m_0 r^2\dot{\phi}_2^2 - m_0\dot{y}_2\dot{\phi}_2 r cos\phi_2 - m_0 r\dot{\phi}_1\dot{\phi}_2 L_2\cos(\phi_2 - \phi_1) + \frac{1}{2}m_1\dot{y}_1^2 + \frac{1}{2}m_0 L_2^2\dot{\phi}_1^2 - \frac{1}{2}K_1\left(y_1^2 - 2y_1 y_{e1} + y_{e1}^2\right)^2 + \frac{1}{2}K_2\left(y_1^2 - 2y_1 y_2 + y_1^2\right)^2 + \frac{1}{2}K_T\phi_1^2 \quad (28)$$

For the application of the Lagrange Equation, the generalized coordinates of the system in question must be determined. For the system of the present work, the following generalized coordinates are defined: y_1, y_2, ϕ_1 and ϕ_2, so according to the Lagrange Equation, the Lagrangian (Eq. 16) must be derived in relation to these generalized coordinates.

But, once the equations of kinetic, potential and dissipation energies are deduced, the Hamilton Principle can be used for each one of the generalized coordinates. As will be shown below: For the y_1 coordinate, vertical displacement of the tire:

$$\begin{aligned} &\frac{d}{dt}\left(\frac{\partial L}{\partial \dot{y}_1}\right) - \left(\frac{\partial L}{\partial y_1}\right) = Q_1 \\ &\frac{d}{dt}\left(\frac{\partial T_T}{\partial \dot{y}_1} - \frac{\partial V_T}{\partial \dot{y}_1}\right) - \left(\frac{\partial T_T}{\partial y_1} - \frac{\partial V_T}{\partial y_1}\right) = Q_1 \end{aligned} \quad (29)$$

But: $\frac{\partial V_T}{\partial \dot{y}_1} = 0$ e $\frac{\partial T_T}{\partial y_1} = 0$ so the previous equation looks like this:

$$\frac{d}{dt}\left(\frac{\partial T_T}{\partial \dot{y}_1}\right) + \frac{\partial V_T}{\partial y_1} = Q_1$$

$$m_1\ddot{y}_1 = -K_1(y_1 - y_{e1}) + K_2(y_2 - y_1) + C(\dot{y}_2 - \dot{y}_1) - \delta z \quad (30)$$

where z is the evolutionary variable given by:

$$\dot{z} = -\gamma|\dot{y}_2 - \dot{y}_1|z|z|^{n-1}z - \beta(\dot{y}_2 - \dot{y}_1)|z|^n + \lambda(\dot{y}_2 - \dot{y}_1)$$

More details on the evolutionary variable z [5].

And *ye1* is considered to be an excitation of the harmonic type and given as follows $y_{e1} = Acos(wt)$, where A is the amplitude that represents the irregularities of the ground surface.

For the y_2 coordinate, vertical displacement of the chassis:

$$\begin{aligned} &\frac{d}{dt}\left(\frac{\partial L}{\partial \dot{y}_2}\right) - \left(\frac{\partial L}{\partial y_2}\right) = Q_2 \\ &\frac{d}{dt}\left(\frac{\partial T_T}{\partial \dot{y}_2} - \frac{\partial V_T}{\partial \dot{y}_2}\right) - \left(\frac{\partial T_T}{\partial y_2} - \frac{\partial V_T}{\partial y_2}\right) = Q_2 \end{aligned} \quad (31)$$

But: $\frac{\partial V_T}{\partial \dot{y}_2} = 0$ e $\frac{\partial T_T}{\partial y_2} = 0$ so the previous equation looks like this:

$$\frac{d}{dt}\left(\frac{\partial T_T}{\partial \dot{y}_2}\right) + \frac{\partial V_T}{\partial y_2} = Q_2$$

$$\begin{aligned}&(m_2 + m_3 + m_0)\ddot{y}_2 - (m_3 + m_0)L_2\ddot{\phi}_1 sin\phi_1 + m_0 r\ddot{\phi}_2 cos\phi_2 \\ &= (m_3 + m_0)L_2\dot{\phi}_1^2 cos\phi_1 + m_0 r\dot{\phi}_2^2 sin\phi_2 + K_2(y_2 - y_1) + \\ &C(\dot{y}_1 - \dot{y}_2) - \delta z\end{aligned} \tag{32}$$

Similarly, the Hamilton Principle is used for the ϕ_1 coordinate, angular displacement of the tower:

$$\begin{aligned}&\tfrac{d}{dt}\left(\tfrac{\partial L}{\partial \dot{\phi}_1}\right) - \left(\tfrac{\partial L}{\partial \phi_1}\right) = Q_3 \\ &\tfrac{d}{dt}\left(\tfrac{\partial T_T}{\partial \dot{\phi}_1} - \tfrac{\partial V_T}{\partial \dot{\phi}_1}\right) - \left(\tfrac{\partial T_T}{\partial \phi_1} - \tfrac{\partial V_T}{\partial \phi_1}\right) = Q_3\end{aligned} \tag{33}$$

But: $\frac{\partial V_T}{\partial \dot{\phi}_1} = 0$ so the previous equation looks like this:

$$\frac{d}{dt}\left(\frac{\partial T_T}{\partial \dot{\phi}_1}\right) - \frac{\partial T_T}{\partial \phi_1} + \frac{\partial V_T}{\partial \phi_1} = Q_3$$

$$\begin{aligned}&-(m_3 + m_0)\ddot{y}_2 L_2 sin\phi_1 + 2m_3 L_2^2\ddot{\phi}_1 + m_0 L_2^2\ddot{\phi}_1 - \\ &m_0 r L_2\ddot{\phi}_2 \cos(\phi_2 - \phi_1) = -m_0 r L_2\dot{\phi}_2 \sin(\phi_2 - \phi_1)\left(\dot{\phi}_2 - \dot{\phi}_1\right) - \\ &m_0 r L_2\dot{\phi}_2\dot{\phi}_1 \sin(\phi_2 - \phi_1) - K_T\phi_1 - C_T\dot{\phi}_1\end{aligned} \tag{34}$$

And now, using Hamilton's Principle for the ϕ_2 coordinate, angular displacement of the unbalanced mass, we have:

$$\begin{aligned}&\tfrac{d}{dt}\left(\tfrac{\partial L}{\partial \dot{\phi}_2}\right) - \left(\tfrac{\partial L}{\partial \phi_2}\right) = Q_4 \\ &\tfrac{d}{dt}\left(\tfrac{\partial T_T}{\partial \dot{\phi}_2} - \tfrac{\partial V_T}{\partial \dot{\phi}_2}\right) - \left(\tfrac{\partial T_T}{\partial \phi_2} - \tfrac{\partial V_T}{\partial \phi_2}\right) = Q_4\end{aligned} \tag{35}$$

But: $\frac{\partial V_T}{\partial \dot{\phi}_2} = 0$ so the previous equation looks like this:

$$\begin{aligned}&\tfrac{d}{dt}\left(\tfrac{\partial T_T}{\partial \dot{\phi}_2}\right) - \tfrac{\partial T_T}{\partial \phi_2} + \tfrac{\partial V_T}{\partial \phi_2} = Q_4 \\ &2m_0 r^2\ddot{\phi}_2 + m_0 r\ddot{y}_2 cos\phi_2 - m_0 r L_2\ddot{\phi}_1 cos(\phi_2 - \phi_1) \\ &= -m_0 r L_2\dot{\phi}_1 \sin(\phi_2 - \phi_1)\left(\dot{\phi}_2 - \dot{\phi}_1\right) + \\ &m_0 r L_2\dot{\phi}_1\dot{\phi}_2 \sin(\phi_2 - \phi_1) + \left(\hat{a} - \hat{b}\dot{\phi}_2\right)\end{aligned} \tag{36}$$

So the system of differential equations that define the movements of the system under

$$\begin{aligned}m_1\ddot{y}_1 &= -K_1(y_1 - y_{e1}) + K_2(y_2 - y_1) + C(\dot{y}_2 - \dot{y}_1) - \delta z \\ &(m_2 + m_3 + m_0)\ddot{y}_2 - (m_3 + m_0)L_2\ddot{\phi}_1 sin\phi_1 + m_0 r\ddot{\phi}_2 cos\phi_2\end{aligned}$$

$$
\begin{aligned}
&= (m_3 + m_0)L_2\dot{\phi}_1^2 cos\phi_1 + \\
&m_0 r\dot{\phi}_2^2 sin\phi_2 + K_2(y_2 - y_1) + C(\dot{y}_1 - \dot{y}_2) - \delta z \\
&\quad - (m_3 + m_0)\ddot{y}_2 L_2 sin\phi_1 + 2m_3 L_2^2\ddot{\phi}_1 + m_0 L_2^2\ddot{\phi}_1 \\
&\quad - m_0 r L_2\ddot{\phi}_2 \cos(\phi_2 - \phi_1) = - \\
&m_0 r L_2\dot{\phi}_2 \sin(\phi_2 - \phi_1)\left(\dot{\phi}_2 - \dot{\phi}_1\right) \\
&\quad - m_0 r L_2\dot{\phi}_2\dot{\phi}_1 \sin(\phi_2 - \phi_1) - K_T\phi_1 - C_T\dot{\phi}_1 \\
&2m_0 r^2\ddot{\phi}_2 + m_0 r\ddot{y}_2 cos\phi_2 - m_0 r L_2\ddot{\phi}_1 cos(\phi_2 - \phi_1) \\
&= -m_0 r L_2\dot{\phi}_1 \sin(\phi_2 - \phi_1)\left(\dot{\phi}_2 - \dot{\phi}_1\right) + \\
&m_0 r L_2\dot{\phi}_1\dot{\phi}_2 \sin(\phi_2 - \phi_1) + \left(\hat{a} - \hat{b}\dot{\phi}_2\right)
\end{aligned}
\tag{37}
$$

When the turret plus the non-ideal unbalanced motor are considered as a simple pendulum, then the angle ϕ_1 is considered small compared to ϕ_2. Therefore, the following relation is valid [13].

$$
\begin{cases}
sin\phi_1 \cong \phi_1 \\
cos\phi_1 \cong 1
\end{cases}
$$

Thus, the system of equations presented above (Eq. 37) is rewritten as follows:

$$
\begin{aligned}
&m_1\ddot{y}_1 \\
&\quad = -K_1(y_1 - y_{e1}) + K_2(y_2 - y_1) + C(\dot{y}_2 - \dot{y}_1) - \delta z \\
&\quad (m_2 + m_3 + m_0)\ddot{y}_2 - (m_3 + m_0)L_2\ddot{\phi}_1\phi_1 + m_0 r\ddot{\phi}_2 cos\phi_2 \\
&\quad = (m_3 + m_0)L_2\dot{\phi}_1^2 + \\
&\quad m_0 r\dot{\phi}_2^2 sin\phi_2 + K_2(y_2 - y_1) + C(\dot{y}_1 - \dot{y}_2) - \delta z \\
&\quad\quad - (m_3 + m_0)\ddot{y}_2 L_2\phi_1 + 2m_3 L_2^2\ddot{\phi}_1 + m_0 L_2^2\ddot{\phi}_1 \\
&\quad\quad - m_0 r L_2\ddot{\phi}_2 \cos(\phi_2 - \phi_1) = - \\
&\quad m_0 r L_2\dot{\phi}_2 \sin(\phi_2 - \phi_1)\left(\dot{\phi}_2 - \dot{\phi}_1\right) \\
&\quad\quad - m_0 r L_2\dot{\phi}_2\dot{\phi}_1 \sin(\phi_2 - \phi_1) - K_T\phi_1 - C_T\dot{\phi}_1 \\
&\quad 2m_0 r^2\ddot{\phi}_2 + m_0 r\ddot{y}_2 cos\phi_2 - m_0 r L_2\ddot{\phi}_1 cos(\phi_2 - \phi_1) \\
&\quad = -m_0 r L_2\dot{\phi}_1 \sin(\phi_2 - \phi_1)\left(\dot{\phi}_2 - \dot{\phi}_1\right) + \\
&\quad m_0 r L_2\dot{\phi}_1\dot{\phi}_2 \sin(\phi_2 - \phi_1) + \left(\hat{a} - \hat{b}\dot{\phi}_2\right)
\end{aligned}
\tag{38}
$$

The previous system of equations (Eq. 38) is rewritten as follows:

$$
\begin{aligned}
&\ddot{y}_1 = -q_1(y_1 - y_{e1}) + q_2(y_2 - y_1) + p_1(\dot{y}_2 - \dot{y}_1) - \mu z \\
&\quad (1 + \alpha_1 + \alpha)\ddot{y}_2 - (\alpha_1 + \alpha)\ddot{\phi}_1\phi_1 + \alpha r\ddot{\phi}_2 cos\phi_2 \\
&\quad = (\alpha_1 + \alpha)L_2\dot{\phi}_1^2 + \\
&\quad \alpha r\dot{\phi}_2^2 sin\phi_2 + q_3(y_2 - y_1) + p_2\left(y_1^{'} - y_2^{'}\right) - \mu_1 z
\end{aligned}
$$

$$
\begin{aligned}
&-\frac{m_3+m_0}{2m_3L_2}\ddot{y}_2\phi_1+\left(1+\frac{m_0}{2m_3}\right)\ddot{\phi}_1-\frac{m_0r}{2m_3L_2}\ddot{\phi}_2\cos(\phi_2-\phi_1)=-\\
&\frac{m_0r}{2m_3L_2}\dot{\phi}_2\sin(\phi_2-\phi_1)\left(\dot{\phi}_2-\dot{\phi}_1\right)\\
&-\frac{m_0r}{2m_3L_2}\dot{\phi}_2\dot{\phi}_1\sin(\phi_2-\phi_1)-q_4\phi_1-p_3\dot{\phi}_1\\
&\frac{1}{2r}\ddot{y}_2cos\phi_2+\ddot{\phi}_2-\frac{m_0L_2}{2r}\ddot{\phi}_1cos(\phi_2-\phi_1)\\
&=\frac{L_2}{2r}\dot{\phi}_1\sin(\phi_2-\phi_1)\left(\dot{\phi}_2-\dot{\phi}_1\right)+\\
&\frac{L_2}{2r}\dot{\phi}_1\dot{\phi}_2\sin(\phi_2-\phi_1)+a-b\dot{\phi}_2
\end{aligned}
\tag{39}
$$

The parameters considered in the previous system are listed below:

$$
\begin{aligned}
q_1=\tfrac{K_1}{m_1}, q_2=\tfrac{K_2}{m_1}, q_3=\tfrac{K_2}{m_1}, q_3=\tfrac{K_2}{m_2}, p_1=\tfrac{C}{m_1}, p_2=\tfrac{C}{m_1}, p_3=\tfrac{C_T}{m_3L_2^2}, \alpha=\tfrac{m_0}{m_2}\alpha_1=\tfrac{m_3}{m_2},\\
\alpha_2=\tfrac{m_0}{m_3}, \zeta=\tfrac{r}{L_2}, \mu=\tfrac{\delta}{m_1L_2}, \mu_1=\tfrac{\delta}{m_2L_2}, a=\tfrac{\hat{a}}{m_0r^2}, b=\tfrac{\hat{b}}{m_0r^2}.
\end{aligned}
$$

The system of equations is then rewritten, making use of a change of variables employing the following state variables:

$$
u_1=y_1, u_2=y_1', u_3=y_2, u_4=y_2', u_5=\phi_1, u_6=\phi_2', u_7=\phi_2, u_8=\phi_2',\ \text{e}\, u_9=z.
$$

Which results in a new system of equations:

$$
\begin{cases}
E_1y_2-E_2\phi_1+E_3\phi_2=f_2\\
-E_4y_2+E_5\phi_1+E_6\phi_2=f_3\\
E_7y_2-E_8\phi_1+E_9\phi_2=f_4
\end{cases}
\tag{40}
$$

Where do you have:

$$
\begin{aligned}
f_1&=-q_1[u_1-A\cos(wt)]+q_2(u_3-u_1)+p_1(u_4-u_2)-\mu_1z-u_5)-q_4u_5-p_3u_6\\
f_2&=(\alpha_1+\alpha)L_2u_6^2+\alpha ru_8^2\sin u_7-q_3(u_3-u_1)-p_2(u_4-u_2)+\mu_1z\\
f_3&=-\tfrac{m_0r}{2m_3L_2}u_8\sin(u_7-u_5)(u_8-u_6)-\tfrac{m_0r}{2m_3L_2}u_6u_8\sin(u_7\\
f_4&=-\tfrac{L_2}{2r}u_6\sin(u_7-u_5)(u_8-u_6)+\tfrac{L_2}{2r}u_6u_8\sin(u_7-u_5)+\alpha-bu_8
\end{aligned}
$$

And also:

$$
\begin{aligned}
&E_1=1+\alpha_1+\alpha E_2=(\alpha_1+\alpha_2)L_2u_5E_3=ar\cos(\alpha_7)E_4=\tfrac{m_3+m_0}{2m_3L_2}u_5E_5=1+\tfrac{m_0}{2m_3}\\
&E_6=\tfrac{m_0r}{2m_3L_2}\cos(u_7-u_5)E_7=\tfrac{1}{2r}\cos(u_7)E_8=\tfrac{m_0L_2}{2r}\cos(u_7-u_5)E_9=1
\end{aligned}
$$

So, rewriting the system in matrix form, you have:

$$\begin{bmatrix} E_1 & -E_2 & E_3 \\ -E_4 & E_5 & -E_6 \\ E_7 & -E_8 & E_9 \end{bmatrix} \begin{bmatrix} y_2^{"} \\ \phi_1^{"} \\ \phi_2^{"} \end{bmatrix} = \begin{bmatrix} f_2 \\ f_3 \\ f_4 \end{bmatrix}$$

$$\begin{bmatrix} y_2^{"} \\ \phi_1^{"} \\ \phi_2^{"} \end{bmatrix} = \begin{bmatrix} f_2 \\ f_3 \\ f_4 \end{bmatrix} \begin{bmatrix} E_1 & -E_2 & E_3 \\ -E_4 & E_5 & -E_6 \\ E_7 & -E_8 & E_9 \end{bmatrix}^{-1} \tag{41}$$

Finally, solving the inverse matrix and making the necessary multiplication of this answer in the system of equations above, we have the system of second order linear differential equations that govern the dynamics of the system under study, presented below:

$$\begin{aligned} y_1 &= f_1 \\ y_2 &= 1/\Delta[(E_5E_9 - E_6E_8)f_2 + (E_2E_9 - E_3E_8)f_3 + (E_2E_6 - E_3E_5)f_4] \\ \emptyset_1 &= 1/\Delta[(E_4E_9 - E_6E_7)f_2 + (E_1E_9 - E_3E_7)f_3 + (E_1E_6 - E_3E_4)f_4] \\ \emptyset_2 &= 1/\Delta[(E_4E_8 - E_5E_7)f_2 + (E_1E_8 - E_2E_7)f_3 + (E_1E_5 - E_2E_4)f_4] \\ z' &= -\gamma|u_4 - u_2|u_9|u_9|^{n-1} - \beta(u_4 - u_2)|u_9|^n + \lambda(u_4 - u_2) \end{aligned} \tag{42}$$

The parameter Δ of the previous equation (Eq. 42) is given by:

$$\Delta = E_1E_5E_9 - E_1E_6E_8 - E_2E_4E_9 + E_2E_6E_7 + E_3E_4E_8 - E_3E_5E_7$$

Making now, the right sides of the equations of $y2''$, $\phi 1''$ and $\phi 2''$ of the previous system (Eq. 42) equal to f_5, f_6 and f_7, respectively, and also the equation of z equal to f_8 as follows:

$$f_8 = -\gamma|u_4 - u_2|u_9|u_9|^{n-1} - \beta(u_4 - u_2)|u_9|^n + \lambda(u_4 - u_2) \tag{43}$$

You can write the derivatives of system 42 as follows:

$$\begin{aligned} u_1' &= u_2 \\ u_2' &= f_1 \\ u_3' &= u_4 \\ u_4' &= f_5 \\ u_5' &= u_6 \\ u_6' &= f_6 \\ u_7' &= u_8 \\ u_8' &= f_7 \\ u_9' &= f_8 \end{aligned} \tag{44}$$

3 Results

3.1 System Responses in Time Domain

Time and phase domain responses will be presented for the following system components: wheel mass, trailer mass, mass concentrated at the top of the tower and unbalanced engine mass, respectively. The values considered for the dimensionless parameters of the system are those shown in Table 1, for a time interval of $0 \leq t \leq 100$ and the initial conditions were considered as being null.

The following table (Table 2) shows the values considered for the MR damper parameters.

Figure 2 shows the behavior of the displacements of the wheel in (a), the trailer in (b), the turret in (c) and the angular velocity of the unbalanced mass of the engine in (d), under suspension action with MR, in red compared to the MR shockless response in black. It can be seen that with the addition of the suspension with MR it significantly reduces the range of motion of each component of the system, having a lesser influence, in relation to the other components, on the displacement of the wheel, as expected. It is verified that the greatest influence is on the displacement of the trailer, which satisfies the proposed objectives, since the proposal is the reduction of the amplitudes of the trailer and the tower.

Table 1 Values for dimensionless parameters for the non-suspension system with MR

Parameter	Value	Parameter	Value
q1	77.5	α1	0.247
q2	6.016	b	1.3
q3	1.11	μ	500
q4	5.395	μ1	92.307
p1	1.306	α	7.69 × 10–4
p2	0.241	p3	0.108

Table 2 Values assigned to the parameters related to the MR damper

Parameter	Value
γ (1/m2)	800
β (1/m2)	1,000,000
λ	1.0
n	2.0

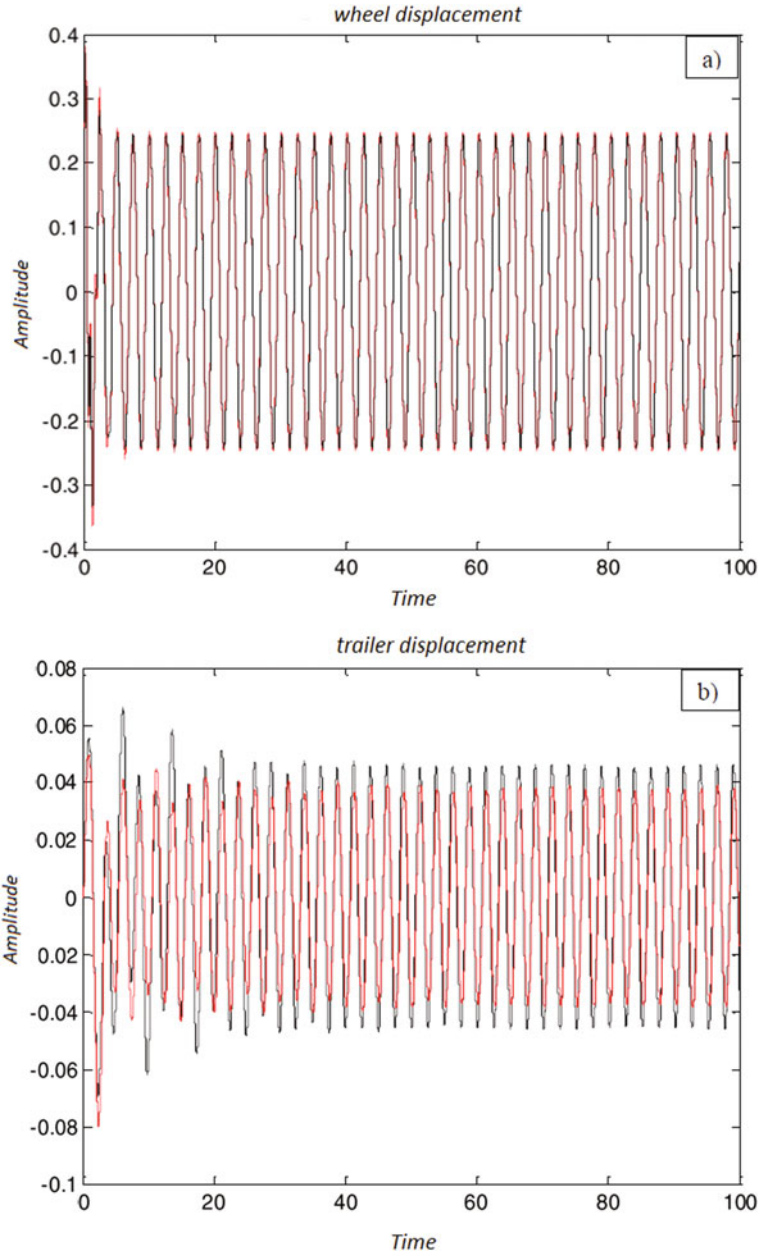

Fig. 2 displacements of the wheel in (**a**), the trailer in (**b**), the turret in (**c**) and the angular velocity of the unbalanced mass of the engine in (**d**)

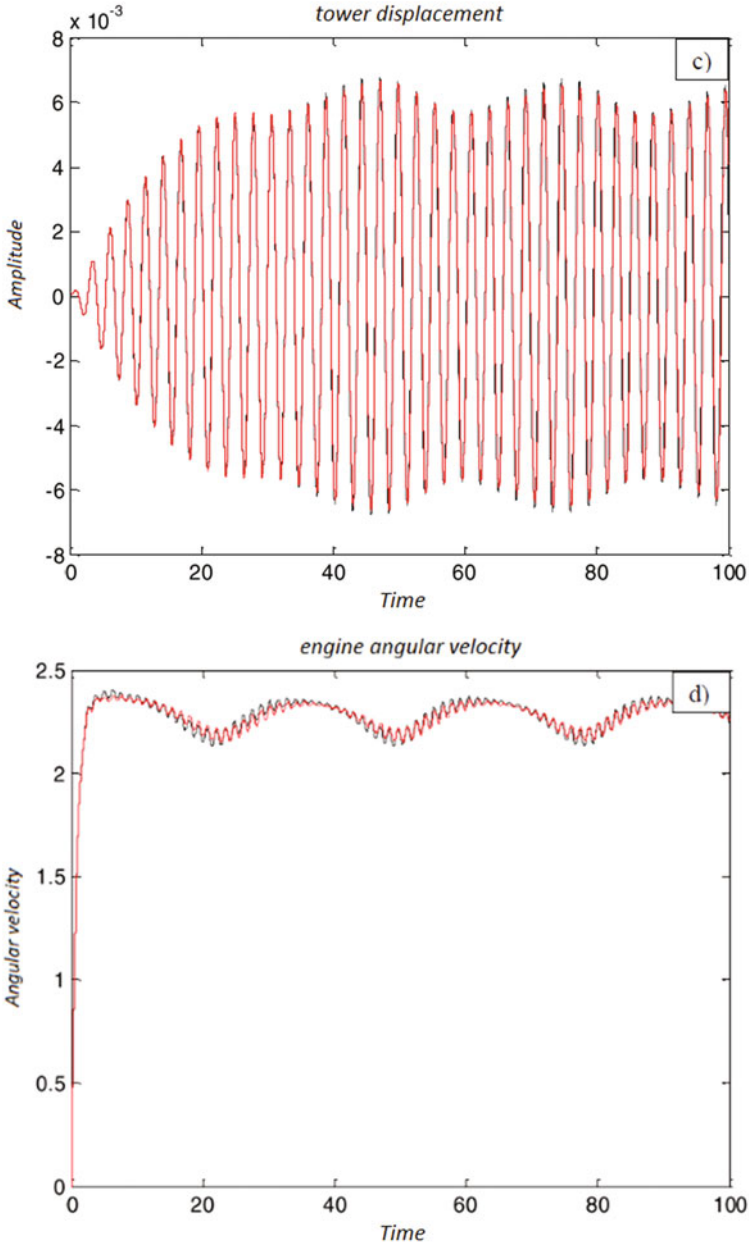

Fig. 2 (continued)

3.2 *Analyze the Influence of the External Force Applied on the Structure Described*

We analyze the influence of the external force applied on the structure described by Eq. (42) considering amplitude A in the interval [0.1: 0.3] and frequency ω in the interval [1, 2]. For this we use the 4th order Runge–Kutta method with an integration step h = 0.001 and a total integration time t = 106[s]. We also consider a transient time of 40% of the total time and considering the initial conditions × 0 = [0, 0, 0, 0, 0, 0, 0, 0, 0, 0]. Figure 3a represents the maximum amplitude of the displacement of the trailer and Fig. 3b of the tower that supports the motor for spraying, both are described by the set of Eq. 42. Thus, the yellow regions represent the maximum amplitude and the light gray region represents the minimum amplitude for the structure.

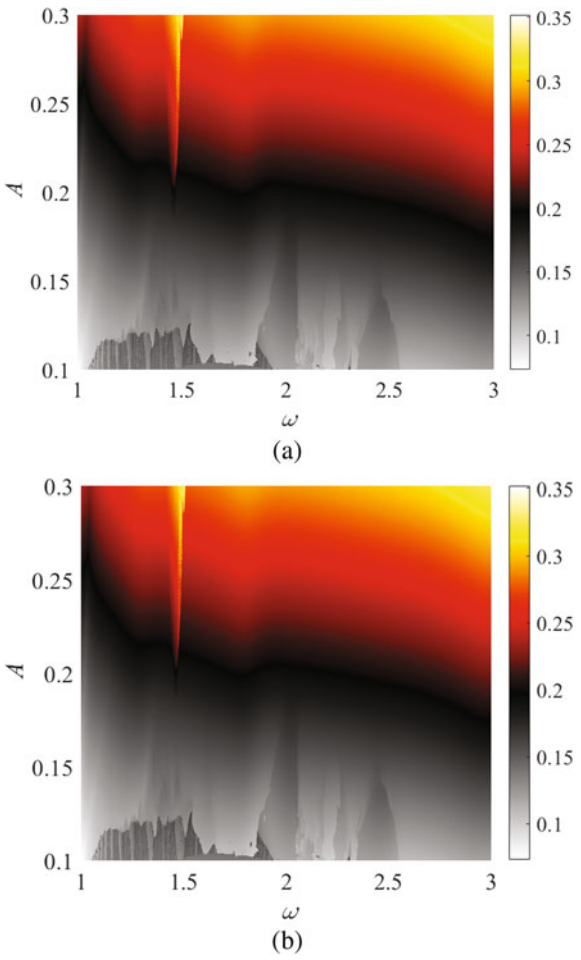

Fig. 3 Representation of the maximum amplitude considering Eq. (42). **a** trailer displacement and **b** turret displacement

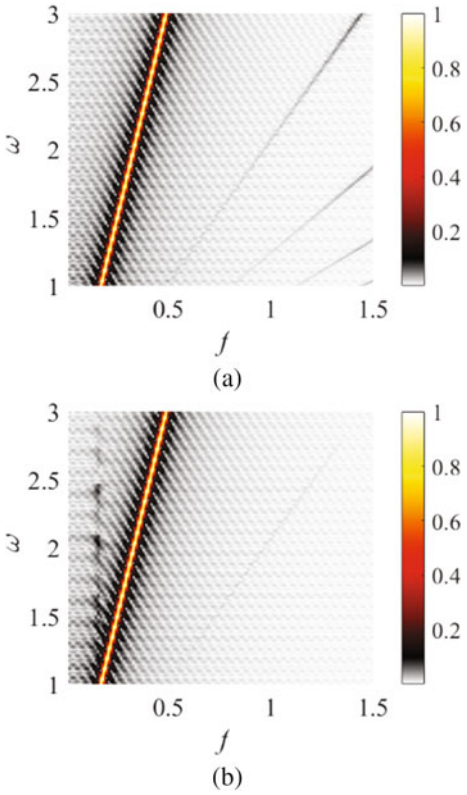

Fig. 4 Representation of the FFT for the parameter ω as Eq. (42). **a** trailer displacement and **b** turret displacement

Another analysis performed was the oscillation frequency and thus we obtain the fast Fourier transforms (FFT) with the variation of the amplitude of the external force (ω), in which we can observe a characteristic frequency of the Eq. (42) referring to the trailer and the tower. Figure 4. (a) represents the FFT sweeping the parameter ω in the interval [1, 2] of the trailer displacement, in which we can observe a natural frequency of the system in yellow and in gray scale are very low secondary frequencies. In Fig. 4b represents the variation ω for the same interval, however, for the tower displacement, in yellow it represents the dominant frequency of the system and in gray, low amplitude secondary frequencies.

Therefore, we delimited the maximum amplitude regions for the displacement of the sprayer system truck and tower considering the external force applied to the system. This external force in Eq. (42) represents possible irregularities in the terrain where the spraying vehicle moves, as high displacements in the structure compromise the spraying application. The analysis of the frequency of for the parameter ω showed that there is a natural frequency for both the truck and the tower vibration, which showed a behavior of possible periodicity, such frequencies are between 0.1 and 0.5 [Hz]. Thus, Fig. 5a–c represent the time series of the trailer displacement for $\omega = 2.936$ [Hz] and considering $A = [0.0, 0.16, 0.5]$, respectively.

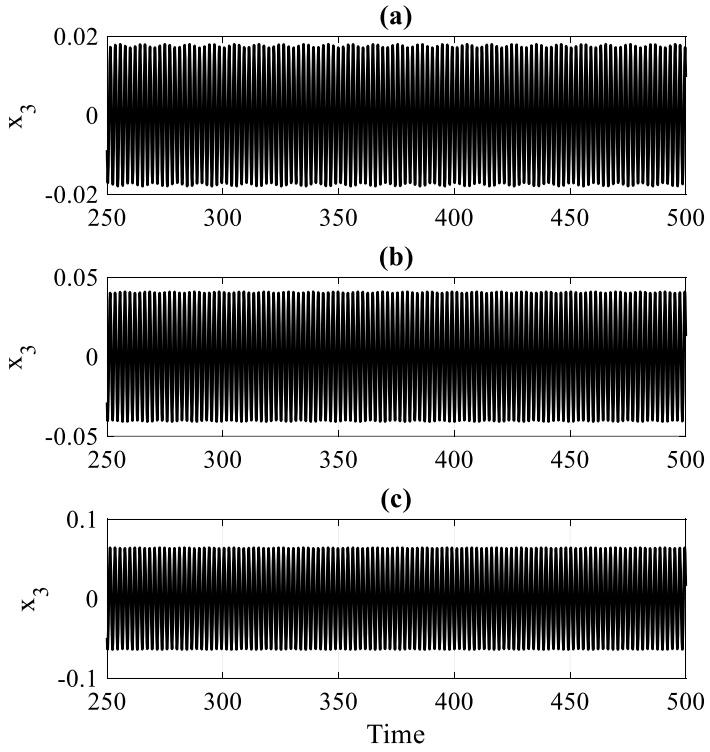

Fig. 5 Time series of the trailer displacement **a** A = 0.0, **b** A = 1.6 and **c** A = 0.5

Thus, Figs. 6a–c represent the time series of the trailer displacement for $\omega = 2.936$ [Hz] and considering A = [0.0, 0.16, 0.5], respectively.

3.3 Calculation of Resulting Vibrations with and Without MR

Thus, we calculated the vibrations resulting from the absence of the MR actuation in Eq. (42), considering the same constants of the previous case, that is, the same constants of the MR system actuation in the vehicle system. Fig. 7a represent the maximum amplitude of the tower and (7b) represent the maximum amplitude of the trailer with the variation of the parameters of the external force of the system. Colors from white to black represent the minimum to medium span and from black to yellow the medium to maximum span.

We also calculated the variation of the control parameter (a) for the system with and without MR application. Thus, Fig. 8a represents the behavior of the tower vibrations with the MR and Fig. 8b without the MR acting on the system with the variation of the parameter a = [3, 7]. It can be observed that there are peaks of

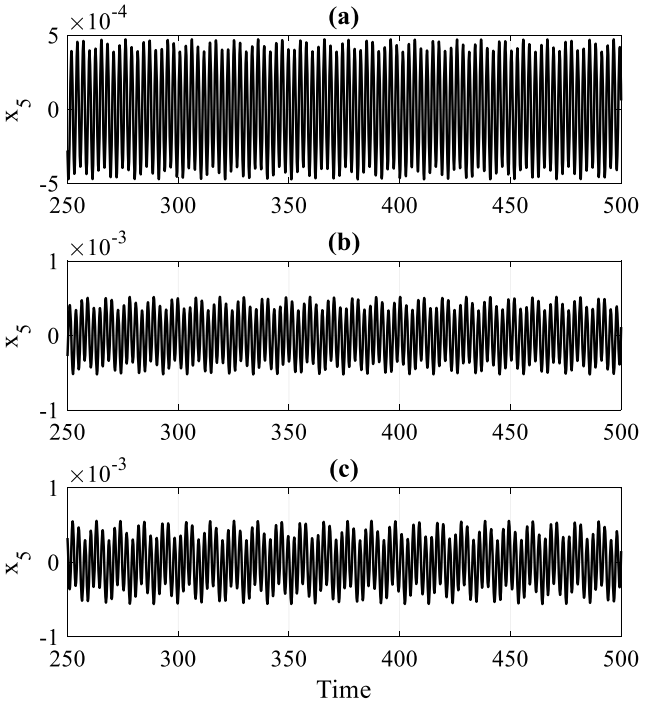

Fig. 6 Time series of tower displacement **a** A = 0.0, **b** A = 1.6 and **c** A = 0.5

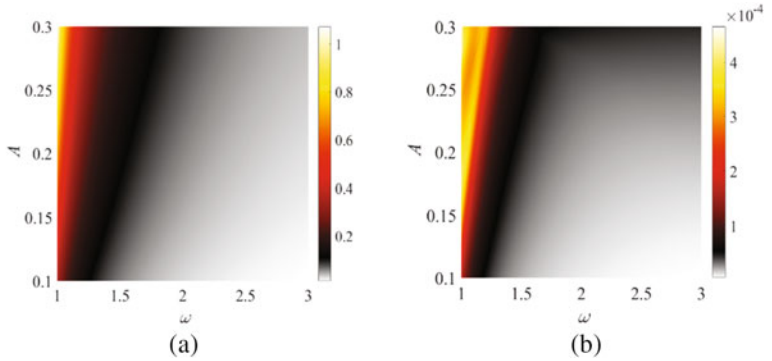

Fig. 7 Representation of maximum amplitude as a function of external force parameters. **a** turret and **b** cart

maximum amplitude a = 5.329 and a = 7.691 for the system containing the MR and for the system with the MR there is a decay of the amplitude, however, it remains in a range from 0.04625 to 0.04616.

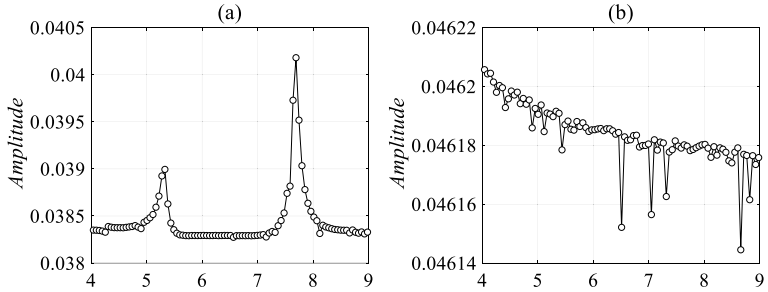

Fig. 8 Representation of the maximum amplitude with the variation of the tower control parameter. **a** with the application of the MR and **b** without the application of the MR

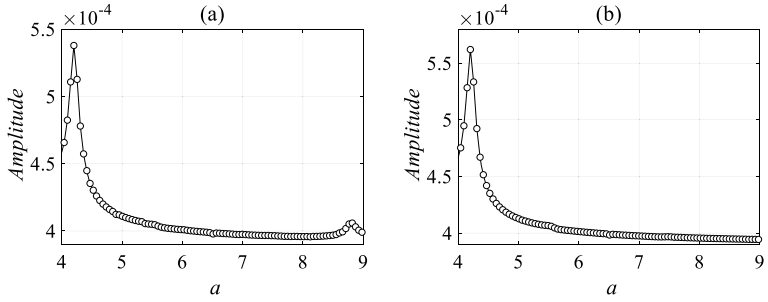

Fig. 9 Representation of the maximum amplitude with the variation of the trailer control parameter. **a** with the application of the MR and **b** without the application of the MR.

And figs. a and fig. B. Represents the behavior of the control parameter (a) for the trailer with and without the MR application, respectively (Fig. 9).

We can observe that there is a peak with maximum amplitude for the value of a = 4.2 in both cases with and without the MR, however, there is the appearance of a peak with amplitude at a = 8.8.

4 Conclusion

In this work, a vehicular suspension with Magneto Rheological (MR) was used, plus the addition of an unbalanced electric motor on top of the tower of a Quarter-car model that represents the structure of an orchard sprayer, in order to reduce vertical movements. mainly of the trailer or chassis, and also the angular movements of the turret. The use of the MR damper proved to be efficient for the main purpose for which it was used: to reduce the oscillation amplitudes of both the trailer or chassis (m_2) and the tower (m_3). It is clearly seen that there were reductions in amplitude, however in some components of the system, this reduction was minimal, as can be

seen, for the wheel, and also for the tower. This fact can be justified due to the shock absorber with MR being strongly influenced by an external electric current, which was considered to be constant in this work. The analysis of the unbalanced electric motor showed that the m_3 mass amplitudes are strongly influenced by a possible unbalance of the sprayer fan blades.

References

1. Balthazar, J.M. et.al.: Vibration Engineering and Technology of Machinery**.** Part of the Mechanisms and Machine Science book series (Mechan. Machine Science), vol. 95. Springer
2. Bombard, A.J.F., Joekes, I., Knobel, M.: Evaluation of a Magneto-Rheological Fluid in a Prototype Damper. Society of Automotive Engineers, Magneto-Rheometer and Magnetometer (2000)
3. Soize, C.: Stochastic modeling of uncertainties in computational structural dynamics—recent theoretical advances. J. Sound Vib. **332**, 2379–2395 (2013)
4. Carlson, J. D.: Controlling Vibration with Magnetorheological Fluid Damping. Lord Corporation. Disponível em: http://www.sensorsmag.com/sensors/electric-magnetic/controlling-vibration-with-magnetorheological-fluid-damping-999. Acesso em: 10 set. 2013 (2002)
5. Cézar, É.S.: Control System Methodology For A Vehicle Suspension With Rheological Magnet (Mr) For A Tower-Type Sprayer (2014). Thesis (Master's degree), Federal University of Pampa
6. Cunha Jr, A., Felix, J. L. P., Balthazar, J. M.: Quantification of parametric uncertainties induced by irregular soil loading in orchard tower sprayer nonlinear dynamics. J. Sound Vibrat. JCR, **408**, 252–269 (2017)
7. Cunha Jr, Nasser, R., Sampaio, R., Lopes, H., Breitman, K.: Uncertainty quantification through Monte Carlo method in a cloud computing setting. Comput. Phys. Commun. **185**, 1355–1363 (2014)
8. Cunha Jr, A., Felix, J.L.P., Balthazar, J.M.: On the nonlinear dynamics of an inverted double pendulum over a vehicle suspension subjected to random excitations. HAL Id: hal-01473586 https://hal.archives-ouvertes.fr/hal-01473586. Submitted on 22 Feb 2017
9. Jansen, L.M., Dyke, S.J.: Semi-active control strategies for MR dampers: A comparative study. ASCE J. Eng. Mech. **126**(8), 795–803 (2000)
10. Kciuk, M., Turczyn, R.: Properties and application of magnetorheological fluids. J. Achieve. Mater. Manuf. Eng. **18**, 127–130 (2006)
11. Kim, J.-H., Oh, J.-H.: Development of an above knee prosthesis using MR Damper and leg simulator. International Conference on Robotics & Automation, pp. 3686- 3691 (2001)
12. Palacios Felix, J. L.: Teoria de Sistemas Vibratórios Aporticados Não Lineares e Não Ideais, p. 205. Tese (Doutorado em Engenharia Mecânica)-Universidade Estadual de Campinas, Faculdade Engenharia Mecânica, Campinas (2002)
13. Sartori, S. Jr., Balthazar, J. M., Pontes, B. R.: Nonlinear dynamics of an orchard tower sprayer based on a double inverted pendulum model.19th International Congress of Mechanical Engineering, Brasilia (2007)
14. Sartori, S. Jr.: Mathematical modeling and dynamic analysis of the tower of an orchard sprayer, p. 150. Dissertation (Masters in Mechanical Engineering) – São Paulo State University "Júlio de Mesquita Filho", Bauru (2008)
15. Sartori, S. Jr., Balthazar, J. M., Pontes, B. R.; Non-linear dynamics of a tower orchard sprayer based on an inverted pendulum model. Biosystems Engineering, pp. 417–426 (2009)
16. Spencer Jr., B. F., Dyke, S. J., Sain, M. K., Carlson, J. D.: Phenomenological model for magnetorheological dampers. J. Eng. Mech. **123**, 230–238 (1997)

17. Tusset, A. M.: Optimal Control Applied in a Non-Linear Vehicle Suspension Model Controlled by Magneto-Rheological Damper, p. 156. Thesis (Doctorate in Engineering)–Federal University of Rio Grande do Sul, PROMEC, Porto Alegre (2008)
18. Tusset, A. M., Balthazar, J. M., Felix, J. L. P.: On elimination of chaotic behavior in a non-ideal portal frame structural system, using both passive and active controls. J. Vibration Control (2012)